

# Unlocking Static Polarization and Strain Density Waves in Perovskites by Softening a Hidden Antiferrodistortive Tilt Gradient Mode

Yajun Zhang,<sup>1,2,3</sup> Devesh R. Kripalani,<sup>3</sup> Xu He,<sup>4</sup> Konstantin Shapovalov,<sup>4</sup> Jiyuan Yang,<sup>5</sup> Hongjian Zhao,<sup>6</sup> Shi Liu,<sup>5</sup> Huadong Yong,<sup>1,2,\*</sup> Xingyi Zhang,<sup>1,2,†</sup> Jie Wang,<sup>7</sup> Kun Zhou,<sup>3,‡</sup> and Philippe Ghosez<sup>4</sup>

<sup>1</sup>Key Laboratory of Mechanics on Disaster and Environment in Western China Attached to The Ministry of Education of China, Lanzhou University, Lanzhou 730000, Gansu, China

<sup>2</sup>Department of Mechanics and Engineering Science, College of Civil Engineering and Mechanics, Lanzhou University, Lanzhou 730000, Gansu, China

<sup>3</sup>School of Mechanical and Aerospace Engineering, Nanyang Technological University, Singapore 639798, Singapore

<sup>4</sup>Theoretical Materials Physics, Q-MAT, Université de Liège, B-4000 Liège, Belgium

<sup>5</sup>Department of Physics, School of Science, Westlake University, Hangzhou 310024, China

<sup>6</sup>Key Laboratory of Material Simulation Methods and Software of Ministry of Education, College of Physics, Jilin University, Changchun 130012, China

<sup>7</sup>Department of Engineering Mechanics, Zhejiang University, 38 Zheda Road, Hangzhou 310027, China

Spin density waves (SDWs) represent a fundamental paradigm of spatially modulated order in condensed matter systems, yet their electrical and mechanical analogues—polarization and strain density waves (PDWs and StDWs)—have remained elusive as equilibrium phases. Here, we introduce a general, symmetry-driven strategy to unlock static PDWs and StDWs in perovskites SrTiO<sub>3</sub> and SrMnO<sub>3</sub>. Using first-principles calculations, we uncover a previously overlooked soft antiferrodistortive tilt gradient mode at small- $q$  wavevector in the phonon dispersion of their presumed *Ima2* ground state under moderate tensile strain. Group-theory analysis reveals that a hard polar-acoustic phonon, which intrinsically carries PDWs and StDWs, is improperly destabilized by a trilinear coupling with this modulated tilt mode and an inherently uniform tilt mode. This interaction drives a structural transition from the *Ima2* phase to a novel lower-energy *Pmn2<sub>1</sub>* phase that hosts long-range-ordered PDWs and StDWs. Strikingly, the engineered StDWs in SrMnO<sub>3</sub> activate an electrically tunable SDW via the flexomagnetic effect. These discoveries fundamentally revise the strain-phase diagrams of prototypical perovskites and establish a unified phonon-engineering framework that links modulated phonon instabilities to targeted density-wave order, offering new pathways for designing advanced electromechanical and magnetoelectric functionalities.

*Introduction*—Ferroic materials (ferroelectric (FE), ferromagnetic, ferroelastic) provide fertile ground for emergent quantum phenomena and advanced functionalities [1–10], owing to the strong coupling between lattice, charge, and spin degrees of freedom. Over the past decades, spatially inhomogeneous magnetization, polarization, and strain have emerged as central drivers of exotic behaviors, including unconventional superconductivity [11–13], enhanced piezoelectric responses [14–17], flexoelectricity [18–22], flexophotovoltaic effect [23, 24], and flexomagnetism [25, 26]. The creation and control of such inhomogeneous states has therefore become a key frontier in modern condensed matter physics.

A paradigmatic example of such inhomogeneous order is the spin density waves (SDWs) [27], characterized by periodic magnetization modulations that break symmetry, underpin exotic states like unconventional superconductivity [11], and enable non-volatile memory [28]. By contrast, realizing its electrical and mechanical counterparts, namely static polarization and strain density waves

(PDWs and StDWs) remains an outstanding challenge in ferroic systems. Specifically, we define a StDW as a spontaneous, static modulation exhibiting long-range periodic strain field that parallels charge, spin, and polarization density waves. A major advance came recently with the observation of PDWs in terahertz-driven SrTiO<sub>3</sub> (STO) [29], mediated by a transiently softened polar-acoustic phonon. The experiment confirmed long-standing speculation of fluctuating order in STO [30, 31]. This non-equilibrium realization, however, raises a fundamental and broadly relevant question: can polar-acoustic phonons be intrinsically softened to stabilize static PDWs and StDWs in equilibrium ferroic materials?

Intriguingly, recent experiments on tensile-strained STO membranes have revealed anomalous quantum behavior near the paraelectric–FE phase boundary [32], strongly suggesting the presence of hidden emergent orders not captured by existing theories. Despite extensive theoretical and experimental investigations into the strain–phase diagrams of STO thin films [33–43], direct evidence for softened polar-acoustic modes, the key microscopic precursors of PDWs and StDWs, has remained absent. With recent breakthroughs in atomic-precision strain engineering and freestanding ferroic membranes [17, 32, 44], it is now timely to revisit tensile strain–phase diagrams of STO from an atomic-scale perspective to

\* yonghd@lzu.edu.cn

† zhangxingyi@lzu.edu.cn

‡ kzhou@ntu.edu.sg

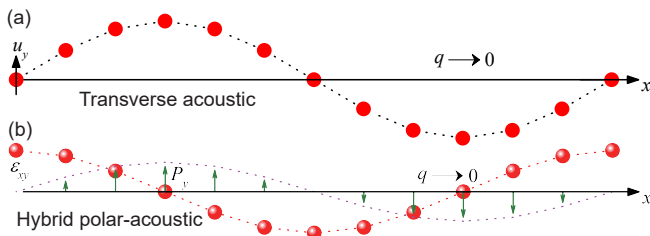


FIG. 1. Schematic of (a) transverse acoustic phonon with modulated atomic displacements, and (b) hybrid polar-acoustic phonon coupling shear strain to polarization propagating along the  $x$  axis. The red circles, red balls, and olive arrows denote the  $y$ -axis displacement, strain, and polarization, respectively.

explore hidden lattice instabilities capable of stabilizing equilibrium modulated ferroic states.

In this Letter, we propose a generic phonon-mediated mechanism for engineering hidden polarization and strain density waves, enabled by a soft antiferrodistortive tilt instability, in stretched STO and SrMnO<sub>3</sub> (SMO) membranes. Our lattice-dynamics analysis reveals a hidden modulated longitudinal tilt instability in the presumed  $Ima2$  ground state of tensile-strained STO and SMO. This modulated tilt mode trilinearly couples with the intrinsically uniform tilt mode and a hard polar-acoustic mode  $\Sigma_2$  with modulated PDWs and StDWs, driving a structural transition to a hitherto unknown, lower-energy  $Pmn2_1$  phase that exhibits spontaneous periodic PDWs and StDWs. Remarkably, in SMO, the engineered StDWs directly activate an emergent SDW with modulated magnetization through the flexomagnetic effect, allowing for electrical tuning of flexomagnetism. More broadly, we reveal that octahedral tilts act as a universal filter, suppressing higher-order harmonics and enforcing clean, single- $q$  modulations, in contrast to the multi- $q$  stripe-like  $a_1/a_2$  90° domain structures of PbTiO<sub>3</sub> (PTO). Our work revises the strain-phase diagram of paradigmatic perovskites STO and SMO and establishes a generic paradigm for unlocking ferroic and antiferrodistortive density waves in functional materials.

*Cross-scale theory of spontaneous PDWs and StDWs.*—The spontaneous emergence of long-range periodic order in polarization and strain constitutes a fundamental challenge. Here, we present a phonon engineering strategy to bridge microscopic lattice dynamics with continuum field theory and unlock long-range polar and elastic modulations in tensile strained STO and SMO. Computational details are provided in the Supplemental Material. [45].

To establish a unified framework, we begin by considering the basic physics of acoustic phonons. A pure transverse acoustic (TA) phonon propagating along the  $x$  axis [Fig. 1(a)] produces a sinusoidal displacement field  $u_y(x) = A \sin(qx)$  [58], which directly induces a periodic shear strain field  $\varepsilon_{xy}(x) = \frac{1}{2} \frac{\partial u_y}{\partial x} = \frac{Aq}{2} \cos(qx)$ .

In such a TA mode, polarization emerges indirectly as a secondary effect via symmetry breaking or flexoelec-

tricity [59]. A hybrid polar-acoustic phonon at a small wavevector  $q$  is fundamentally different. As sketched in Fig. 1(b), such a mode directly couples shear strain to dipole formation, generating both modulated polarization  $P_y(x) = P_0 \sin(qx + \phi)$  and strain fields from a single soft mode.

This theoretical framework establishes a cross-scale foundation for spontaneous polar and elastic modulations. While such hybrid mode remains stable in bulk perovskites, we discover a previously overlooked unstable antiferrodistortive tilt gradient mode in tensile-strained perovskite membranes such as STO and SMO, which, through symmetry-allowed coupling, provides a generic mechanism to activate otherwise stable polar-acoustic modes, driving the formation of long-range ordered density waves (Fig. 2).

*Improper PDWs and StDWs in STO membranes.*—STO, a prototypical incipient ferroelectric known for its pronounced strain-phonon coupling, serves as a model system for exploring strain-induced ferroelectricity [33–43]. Extensive theoretical studies including Ginzburg–Landau–Devonshire phenomenology [40], phase-field simulations [41, 42], deep potential molecular dynamics [43], and first-principles calculations [37–39] have established a consistent phase transition for STO under tensile strain. Taking 1.5% biaxial tensile strain as an example, the high-temperature reference  $P4/mmm$  phase (the cubic structure under in-plane biaxial strain) exhibits two main lattice instabilities in its phonon spectrum shown in Fig. 2(a): unstable polar modes at the  $\Gamma$  point corresponding to in-plane FE distortions  $P_x$  [Fig. 2(b)], and unstable antiferrodistortive modes at the  $A$  point  $(1/2, 1/2, 1/2)$  corresponding to oxygen octahedral tilts. Under tensile strain, the  $a^-a^-c^0$  tilt  $R_{xy}$  [Fig. 2(c)] becomes significantly softer than the  $a^0a^0c^-$  pattern, making it the dominant tilt instability. Condensing the  $P_x$  and the octahedral tilt  $R_{xy}$  leads to the widely accepted FE  $Ima2$  ground state [Fig. 2(d)] [37–39].

Contrary to this consensus, we discover a soft phonon branch near the  $\Gamma$  point in the established  $Ima2$  ground state at 1.5% tensile strain [Fig. 2(e)], indicating a hitherto overlooked instability toward a distinct low-energy modulated phase. Symmetry analysis identifies the unstable eigenmode as mixed modes combining a modulated longitudinal tilt mode  $S_1$  (Irrep  $S_1$ ) and a hybrid polar-acoustic mode  $\Sigma_2$  (Irrep  $\Sigma_2$ ). As schematically depicted in Fig. 2(f), the  $S_1$  component, with  $Amm2$  symmetry, generates a longitudinal tilt modulated at wavevector  $q = (n - 1/2n, n - 1/2n, 0)$  within a  $\sqrt{2}n \times \sqrt{2} \times 2$  supercell. The  $\Sigma_2$  mode ( $Pmc2_1$  symmetry), as shown in Fig. 2(g), induces modulated displacement and polarization fields along the  $x$  axis at  $q = (1/2n, 1/2n, 0)$ . The condensation of these modes and subsequent full structural relaxation within a  $\sqrt{2}n \times \sqrt{2} \times 2$  supercell under 1.5% tensile strain consistently yields a new  $Pmn2_1$  phase [Fig. 2(h)], structurally distinct and energetically favored (Fig. S1 [45]) over the presumed  $Ima2$  ground state.

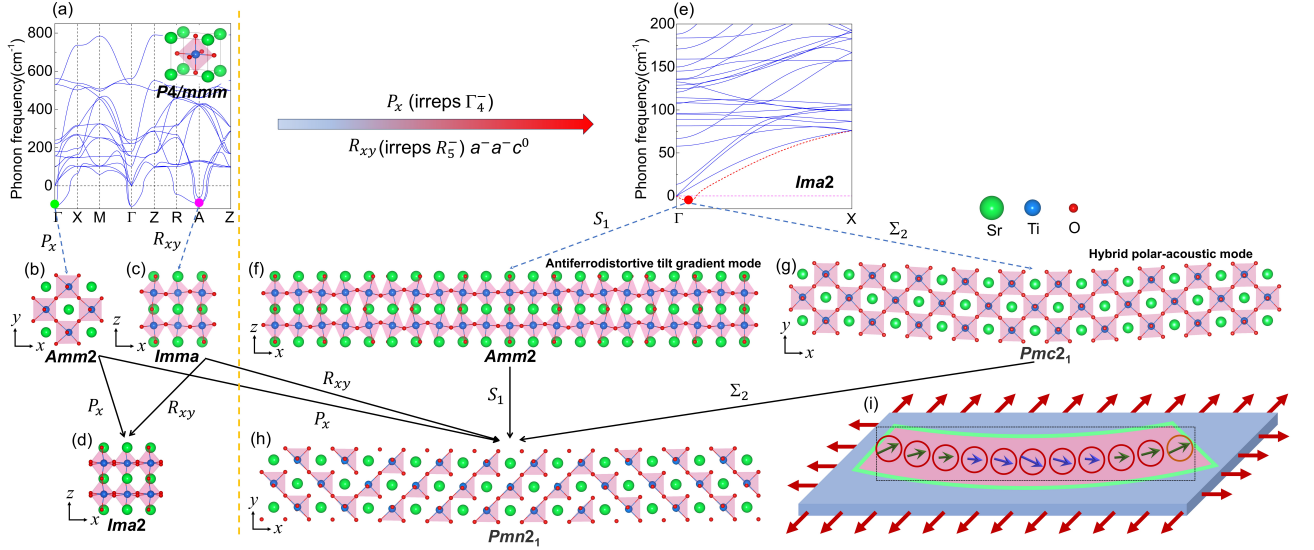


FIG. 2. Atomic theory of spontaneous PDW and StDW. The  $x$ ,  $y$ ,  $z$  axes correspond to  $[110]$ ,  $[1\bar{1}0]$ , and  $[001]$  of the pseudocubic phase. (a) Phonon dispersion of  $P4/mmm$  STO under 1.5% tensile strain; inset shows the corresponding atomic structure. Schematic representations of (b) in-plane polarization  $P_x$ , (c) out-of-phase tilt mode  $R_{xy}$  (projected along  $[1\bar{1}0]$ , with rotation around  $[110]$ ), and (d)  $Ima2$  phase with  $P_x$  and  $R_{xy}$  distortions. (e) Phonon dispersion ( $\Gamma$ -X) of  $Ima2$  STO under the same strain, revealing a hidden instability. (f) Modulated tilt mode  $S_1$  and (g) hybrid polar-acoustic mode  $\Sigma_2$  carrying PDW and StDW. (h) The  $Pmn2_1$  ground state incorporating all four distortions ( $P_x$ ,  $R_{xy}$ ,  $S_1$ ,  $\Sigma_2$ ). (i) Schematic of biaxial tensile strain (brown arrows) inducing PDW and StDW in a freestanding membrane; the arrows in the circles represent the modulated total polarization vectors. The substrate-like layer is a conceptual reference to experimental setups using sacrificial layers, actual DFT calculations use periodic supercells without substrates. The green dashed line separates the conventional understanding (left) from our new findings (right) on the lowest-energy state of STO under moderate tensile strain.

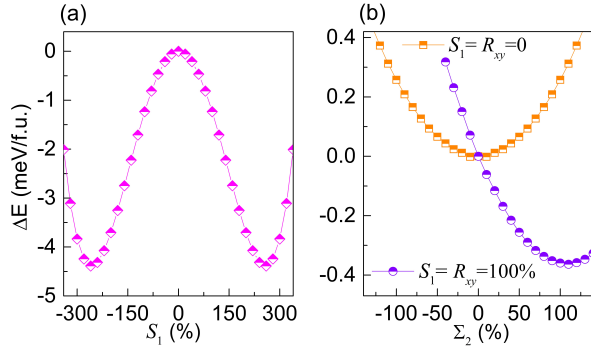


FIG. 3. PESs of the (a)  $S_1$  mode and the (b)  $\Sigma_2$  mode without (orange curve) and with (blue curve) the fixing of  $R_{xy}$  and  $S_1$  modes. Here, 100% denotes the amplitude of distortions in STO under 1.5% tensile strain.

To resolve the stabilization mechanism of this  $Pmn2_1$  phase, we employ group theory symmetry analysis to untangle the symmetry relationships among key distortions ( $P_x$ ,  $R_{xy}$ ,  $S_1$ , and  $\Sigma_2$ ). The potential energy surfaces (PESs) as a function of the normalized mode amplitudes [Fig. 3 and Fig. S2 [45]] show that the  $P_x$ ,  $R_{xy}$ , and  $S_1$  modes exhibit double-well potentials, confirming their roles as primary order parameters, whereas the  $\Sigma_2$  mode displays a single-well potential [Fig. 3(b)], indicating its activation *via* mode coupling. Remarkably, the  $\Sigma_2$  mode

only stabilizes at finite amplitude when both  $R_{xy}$  and  $S_1$  modes are simultaneously condensed [Fig. 3(b) and Figs. S3–S4 [45]]. The linear energy dependence near zero amplitude [Fig. 3(b) and Fig. S5 [45]] for these three modes provides direct symmetry-consistent evidence of a trilinear coupling term:

$$\mathcal{F} = R_{xy}S_1\Sigma_2. \quad (1)$$

The resulting  $Pmn2_1$  phase exhibits pronounced long-range spatial modulations. The octahedral tilt angle displays a cosinusoidal profile [Fig. 4(a)], manifesting as long-range tilt density waves (TDWs). Concurrently, atomic displacements along the  $x$  axis follow a sinusoidal wave profile [Fig. 4(b)], generating a cosinusoidal shear strain wave [Fig. 4(c)] that constitutes a spontaneous StDW. Polarization mapping further reveals a modulated  $P_y$  with identical periodicity [Fig. 4(d)]. The modulated  $P_y$  and uniform  $P_x$  form a coherent PDW, as schematically illustrated in Fig. 2(i). These findings fundamentally revise the tensile strain-phase diagram of STO, establish the  $Pmn2_1$  phase as a versatile platform for hosting trilinear coupling-induced PDW and StDW, and provide a plausible mechanism for anomalous quantum behavior in strained membranes [32].

*Electrically switchable SDW in SMO.*—Flexo-type coupling effects have recently emerged as a critical research

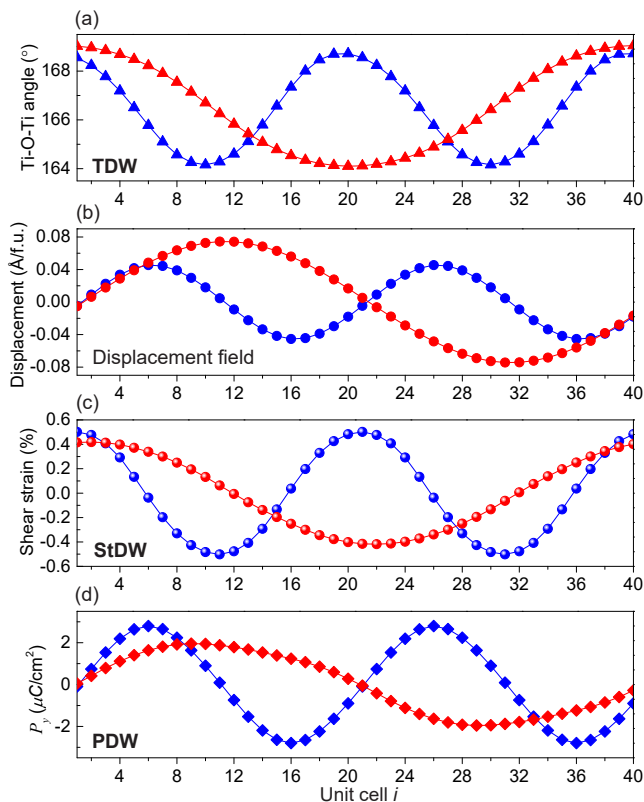


FIG. 4. Improper PDW and StDW in tensile-strained STO. The (a) out-of-plane Ti-O-Ti bond angle, (b) displacement field, (c) strain field, and (d)  $P_y$  along the  $x$  axis. These fields are extracted from the  $10\sqrt{2} \times \sqrt{2} \times 2$  (blue curves) supercell and  $20\sqrt{2} \times \sqrt{2} \times 2$  (red curves) supercell of  $Pmn2_1$  STO under 1.5% tensile strain.

frontier, owing to their great potential for electromechanical and magnetomechanical technologies [18–20, 25, 26]. Although pioneering studies demonstrated flexomagnetic effects [25, 26], their implementation might be hindered by the difficulty of generating deterministic, nanoscale strain gradients via conventional bending methods.

Against this backdrop, we overcome this limitation by leveraging spontaneous StDW in perovskite oxides. While prior first-principles studies consistently identified a tensile strain stabilized  $Ima2$  ground state in SMO [51, 60, 61], we discover that moderate strain stabilizes a modulated  $Pmn2_1$  phase with coexisting PDW and StDW [Fig. 5(a) and S6 [45]], mirroring the behavior in STO. Crucially, this spontaneously generated StDW serves as an ideal built-in platform for producing nanoscale strain gradients, enabling efficient generation of SDW via the flexomagnetic effect.

Within a 3% tensile strained SMO thin film modeled in an  $8\sqrt{2} \times \sqrt{2} \times 2$  supercell, we demonstrate StDW-mediated SDW formation. Figure 5(b) illustrates the sinusoidal strain modulation and cosinusoidal polarization  $P_y$  distribution, analogous to that observed in STO. These modulations directly induce periodic SDW [Fig.

5(c)] with magnetization modulations along the  $x$  axis, the hallmark of the flexomagnetic effect. The SDW period is exactly half that of the strain wave, arising from equivalent magnetization suppression under both positive and negative shear strains (Fig. S7 [45]).

The coexistence of electrically tunable in-plane polarization  $P_x$  and SDW enables direct electric-field control of magnetization. As quantified in Fig. 5(c), the magnetization difference depends on the amplitude and direction of in-plane electric field along the  $x$  axis: a field antiparallel to  $P_x$  enhances the SDW amplitude, whereas a parallel field suppresses it. Beyond a critical field strength, the modulated magnetization is fully quenched [Fig. 5(c)], demonstrating nonvolatile switching off of the StDW-mediated SDW. We thus establish amplitude modulation and non-volatile off switching of StDW-mediated SDW and flexomagnetism via electric fields alone, which offers a direct pathway toward ultra-low-power, voltage-controlled spintronic logic and memory devices.

*PDW/StDW state vs  $90^\circ$  domain.*—The intriguing PDWs and StDWs in modulated long-period STO and SMO stand in stark contrast to those in classical ferroelectrics such as PTO, which under tensile strain form a long-period  $a_1/a_2$   $90^\circ$  domain structure characterized by flattened domains and sharp boundaries [62, 63].

To reconcile these distinct behaviors and establish a unified microscopic description of polarization and strain fields in tensile-strained ferroelectrics, we performed a systematic analysis of the  $\Sigma_2$  mode harmonics across these systems. As summarized in Table 1, multiple  $\Sigma_2$  modes exist relative to the cubic parent structure. In a  $\sqrt{2}n \times \sqrt{2} \times 2$  supercell, each  $\Sigma_2$  mode corresponds to a specific wavevector  $q = (m/2n, m/2n, 0)$ , where  $m$  is an odd integer smaller than  $n$ . The mode with  $q = (1/2n, 1/2n, 0)$  possesses the largest amplitude. The key distinction lies in the strength of the higher-order harmonic modes: STO and SMO exhibit negligible higher-order harmonics, preserving a single- $q$  modulation profile. A similar trend is observed in BFO, where higher-order harmonics are negligible (Table 1), leading to well-ordered, single- $q$  dominant PDWs and StDWs along  $x$  axis (Fig. S8 [45]). In contrast, PTO exhibits strong higher-order harmonics, and the condensation of multiple  $\Sigma_2$  modes gives rise to the anharmonic, stripe-like waveforms shown in Fig. S9 [45].

Under tensile strain, a fundamental microscopic distinction lies in the presence or absence of octahedral tilts, which are inherent in STO, SMO, and BFO but absent in PTO. To clarify the effect of octahedral tilts, we investigate the strain field in Sr-doped PTO grown on a  $\text{DyScO}_3$  substrate. As illustrated in Fig. S10 [45], Sr doping systematically introduces octahedral tilts. If these tilts are neglected in the modeling, multi- $q$  condensation persists, leading to a stripe-like strain and displacement profile within the  $a_1/a_2$  domain structure [Fig. 5(d)]. However, when the Sr-induced tilts are explicitly included, the higher-order harmonics are strongly suppressed (Table 1), driving the system from a multi- $q$  regime toward

TABLE I. Lattice distortions in the modulated FE phase of tensile-strained STO (1.5%), SMO (3%), and BFO (4.5%) membranes, relative to the pseudocubic phase. All values are dimensionless, representing normalized mode amplitudes with respect to the pseudocubic structure. We also list the distortions of PTO and Sr-doped PTO films grown on DyScO<sub>3</sub> substrate.

Compound	Space group	$P_x$	$R_{xy}$	$\Sigma_2, q=1/2n, 1/2n, 0$	$\Sigma_2, q=3/2n, 3/2n, 0$	$\Sigma_2, q=5/2n, 5/2n, 0$	$\Sigma_2, q=7/2n, 7/2n, 0$
STO	$Pmn2_1$	0.122	0.278	0.117	0.001	0.003	0.001
SMO	$Pmn2_1$	0.143	0.205	0.809	0.010	0.008	0.001
BFO	$Pc$	1.235	0.633	0.211	0.002	0.001	0.001
PTO	$Pmc2_1$	0.501	0	1.362	0.192	0.069	0.036
Pb <sub>0.84</sub> Sr <sub>0.16</sub> TiO <sub>3</sub>	$Pmn2_1$	0.580	0.21	0.175	0.005	0	0

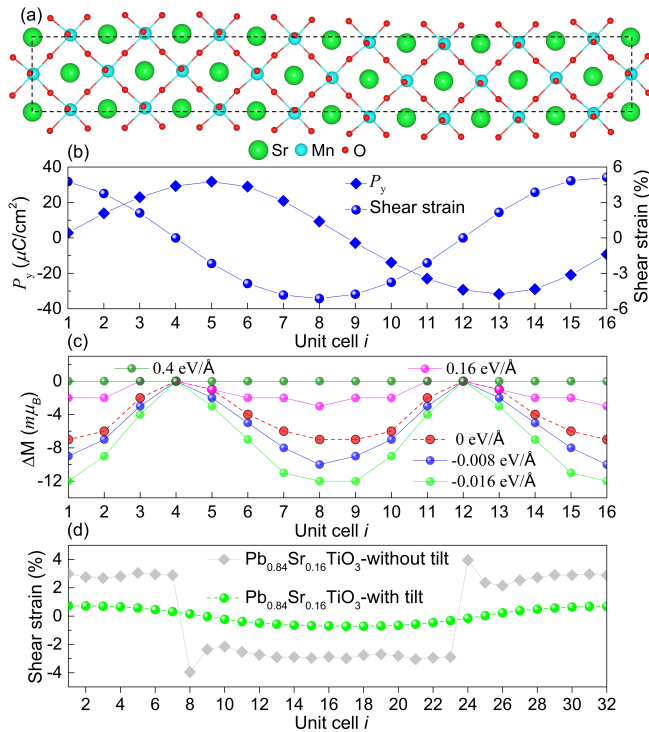


FIG. 5. Electrical and chemical control of density waves. (a) Atomic structure of the low-energy  $Pmn2_1$  phase in  $8\sqrt{2} \times \sqrt{2} \times 2$  SMO supercell under 3% tensile strain. (b) Corresponding global strain field and distribution of  $P_y$  along the  $x$  axis. (c) The spatial distribution of magnetization deviation along the  $x$  axis under different in-plane electric field conditions. (d) Comparison of modulated strain field for  $\text{Pb}_{0.84}\text{Sr}_{0.16}\text{TiO}_3$  grown on the DyScO<sub>3</sub> substrate without and with the involving of tilt distortions, highlighting the critical role of tilt distortions in suppressing higher-order harmonics and stabilizing single- $q$  dominant StDW.

a nearly single- $q$  dominant state [Fig. 5(d)]. Our findings thus establish octahedral engineering as a powerful strategy for tuning density wave states and other functional properties in perovskite oxides *via* selective control of anharmonic mode coupling.

To conclude, the pioneering work of Orenstein et al.

provided the compelling observation of PDWs in STO under ultrafast terahertz excitation, revealing the intrinsically dynamical, nonequilibrium character mediated by flexoelectric coupling. Inspired by this landmark discovery, our work establishes a novel phonon engineering design principle that bridges atomic-scale dynamics with equilibrium polarization and strain modulations in stretched perovskite membranes. We identify a previously overlooked soft antiferrodistortive tilt-gradient mode in tensile-strained STO and SMO. Through a symmetry-allowed improper trilinear coupling with a uniform tilt distortion and a hard polar-acoustic phonon, this hidden instability drives a transition from the presumed  $Ima2$  ground state to a lower-energy, long-period  $Pmn2_1$  phase hosting static PDW and StDW. In SMO, the resulting StDW generates intrinsic nanoscale strain gradients that create a flexomagnetic landscape, enabling direct electric-field control of SDWs and magnetic textures without external mechanical deformation. More broadly, we show that octahedral tilts suppress higher-order polar-acoustic harmonics, favoring single- $q$  dominant modulations, unlike the multi- $q$  domain patterns of classical ferroelectrics such as PTO. This behavior is further confirmed in BFO and Sr-doped PTO, demonstrating the generality of this mechanism across tilted perovskites. Consequently, these results establish a new paradigm for density-wave engineering. Instead of transient, field-driven excitations governed primarily by flexoelectric coupling, the modulated states identified here correspond to stable thermodynamic ground states arising from symmetry-guided trilinear phonon interactions and accessible through static tensile strain. By demonstrating that these long-period modulations can serve as functional parent phases for electrical control of derivative orders such as SDW, our work opens a pathway toward static, electrically controllable multifunctional density-wave phases in complex oxides.

Acknowledgments—Y.Z. acknowledges the financial support received from the National Natural Science Foundation of China (Grant 12472150 and 12432007). Y.Z. also acknowledges the Center for Computational Science and Engineering of Lanzhou University for the computational support provided.

- [1] E. Salje, Phase transitions in ferroelastic and co-elastic crystals, *Ferroelectrics* **104**, 111 (1990).
- [2] A. Devonshire, Theory of ferroelectrics, *Adv. Phys.* **3**, 85 (1954).
- [3] H. Schmid, Multi-ferroic magnetoelectrics, *Ferroelectrics* **162**, 317 (1994).
- [4] E. K. Salje, Ferroelastic materials, *Annu. Rev. Mater. Res.* **42**, 265 (2012).
- [5] L. W. Martin and A. M. Rappe, Thin-film ferroelectric materials and their applications, *Nat. Rev. Mater.* **2**, 1 (2016).
- [6] X. Moya, S. Kar-Narayan, and N. D. Mathur, Caloric materials near ferroic phase transitions, *Nat. Mater.* **13**, 439 (2014).
- [7] W. Eerenstein, N. Mathur, and J. F. Scott, Multiferroic and magnetoelectric materials, *Nature* **442**, 759 (2006).
- [8] M. Fiebig, T. Lottermoser, D. Meier, and M. Trassin, The evolution of multiferroics, *Nat. Rev. Mater.* **1**, 1 (2016).
- [9] J. Junquera, Y. Nahas, S. Prokhorenko, L. Bellaiche, J. Íñiguez, D. G. Schlom, L.-Q. Chen, S. Salahuddin, D. A. Muller, L. W. Martin, *et al.*, Topological phases in polar oxide nanostructures, *Rev. Mod. Phys.* **95**, 025001 (2023).
- [10] A. Schiaffino and M. Stengel, Macroscopic polarization from antiferrodistortive cycloids in ferroelastic srTiO<sub>3</sub>, *Phys. Rev. Lett.* **119**, 137601 (2017).
- [11] P. Dai, J. Hu, and E. Dagotto, Magnetism and its microscopic origin in iron-based high-temperature superconductors, *Nat. Phys.* **8**, 709 (2012).
- [12] S. Hameed, D. Pelc, Z. W. Anderson, A. Klein, R. Spieker, L. Yue, B. Das, J. Ramberger, M. Lukas, Y. Liu, *et al.*, Enhanced superconductivity and ferroelectric quantum criticality in plastically deformed strontium titanate, *Nat. Mater.* **21**, 54 (2022).
- [13] C. Enderlein, J. F. de Oliveira, D. Tompsett, E. B. Saitovitch, S. Saxena, G. Lonzarich, and S. Rowley, Superconductivity mediated by polar modes in ferroelectric metals, *Nat. Commun.* **11**, 4852 (2020).
- [14] Y. Yao, H. Liu, Y. Hu, K. Datta, J. Wu, Y. Zhang, M. G. Tucker, S. Liu, J. C. Neufeind, S. Zhang, *et al.*, Fluctuating local polarization: a generic fingerprint for enhanced piezoelectricity in pb-based and pb-free perovskite ferroelectrics, *Nat. Commun.* **16**, 7442 (2025).
- [15] Z. Kutnjak, J. Petzelt, and R. Blinc, The giant electromechanical response in ferroelectric relaxors as a critical phenomenon, *Nature* **441**, 956 (2006).
- [16] M. Ahart, M. Somayazulu, R. E. Cohen, P. Ganesh, P. Dera, H.-k. Mao, R. J. Hemley, Y. Ren, P. Liermann, and Z. Wu, Origin of morphotropic phase boundaries in ferroelectrics, *Nature* **451**, 545 (2008).
- [17] L. Han, X. Yang, Y. Lun, Y. Guan, F. Huang, S. Wang, J. Yang, C. Gu, Z.-B. Gu, L. Liu, *et al.*, Tuning piezoelectricity via thermal annealing at a freestanding ferroelectric membrane, *Nano Lett.* **23**, 2808 (2023).
- [18] P. Zubko, G. Catalan, and A. K. Tagantsev, Flexoelectric effect in solids, *Annu. Rev. Mater. Res.* **43**, 387 (2013).
- [19] D. Lee, A. Yoon, S. Jang, J.-G. Yoon, J.-S. Chung, M. Kim, J. Scott, and T. Noh, Giant flexoelectric effect in ferroelectric epitaxial thin films, *Phys. Rev. Lett.* **107**, 057602 (2011).
- [20] L. E. Cross, Flexoelectric effects: Charge separation in insulating solids subjected to elastic strain gradients, *J. Mater. Sci.* **41**, 53 (2006).
- [21] P. Zubko, G. Catalan, A. Buckley, P. Welche, and J. Scott, Strain-gradient-induced polarization in srTiO<sub>3</sub> single crystals, *Phys. Rev. Lett.* **99**, 167601 (2007).
- [22] A. Biancoli, C. M. Fancher, J. L. Jones, and D. Damjanovic, Breaking of macroscopic centric symmetry in paraelectric phases of ferroelectric materials and implications for flexoelectricity, *Nat. Mater.* **14**, 224 (2015).
- [23] M.-M. Yang, D. J. Kim, and M. Alexe, Flexophotovoltaic effect, *Science* **360**, 904 (2018).
- [24] L. Shu, S. Ke, L. Fei, W. Huang, Z. Wang, J. Gong, X. Jiang, L. Wang, F. Li, S. Lei, *et al.*, Photoflexoelectric effect in halide perovskites, *Nat. Mater.* **19**, 605 (2020).
- [25] P. Makushko, T. Kosub, O. V. Pylypovskiy, N. Hedrich, J. Li, A. Pashkin, S. Avdoshenko, R. Hübner, F. Ganss, D. Wolf, *et al.*, Flexomagnetism and vertically graded néel temperature of antiferromagnetic Cr<sub>2</sub>O<sub>3</sub> thin films, *Nat. Commun.* **13**, 6745 (2022).
- [26] B. A. Belyaev, A. V. Izotov, P. N. Solovev, and N. M. Boev, Strain-gradient-induced unidirectional magnetic anisotropy in nanocrystalline thin permalloy films, *Phys. Status Solidi. RRL* **14**, 1900467 (2020).
- [27] G. Grüner, The dynamics of spin-density waves, *Rev. Mod. Phys.* **66**, 1 (1994).
- [28] H. Chen, Z. Feng, P. Qin, X. Zhou, H. Yan, X. Wang, Z. Meng, L. Liu, and Z. Liu, Resistive memory based on the spin-density-wave transition of antiferromagnetic chromium, *Phys. Rev. Appl.* **18**, 054046 (2022).
- [29] G. Orenstein, V. Krapivin, Y. Huang, Z. Zhang, G. de la Peña Muñoz, R. A. Duncan, Q. Nguyen, J. Stanton, S. Teitelbaum, H. Yavas, *et al.*, Observation of polarization density waves in SrTiO<sub>3</sub>, *Nat. Phys.* , 1 (2025).
- [30] K. A. Müller, W. Berlinger, and E. Tosatti, Indication for a novel phase in the quantum paraelectric regime of srTiO<sub>3</sub>, *Z. Phys. B* **84**, 277 (1991).
- [31] S. Rowley, L. Spalek, R. Smith, M. Dean, M. Itoh, J. Scott, G. Lonzarich, and S. Saxena, Ferroelectric quantum criticality, *Nat. Phys.* **10**, 367 (2014).
- [32] J. Li, Y. Lee, Y. Choi, J.-W. Kim, P. Thompson, K. J. Crust, R. Xu, H. Y. Hwang, P. J. Ryan, and W.-S. Lee, The classical-to-quantum crossover in the strain-induced ferroelectric transition in srTiO<sub>3</sub> membranes, *Nat. Commun.* **16**, 4445 (2025).
- [33] F. He, B. Wells, and S. Shapiro, Strain phase diagram and domain orientation in SrTiO<sub>3</sub> thin films, *Phys. Rev. Lett.* **94**, 176101 (2005).
- [34] M. P. Warusawithana, C. Cen, C. R. Slesman, J. C. Woicik, Y. Li, L. F. Kourkoutis, J. A. Klug, H. Li, P. Ryan, L.-P. Wang, *et al.*, A ferroelectric oxide made directly on silicon, *Science* **324**, 367 (2009).
- [35] P. Zhang, Q. Li, Z. Li, X. Shi, H. Wang, C. Huo, L. Zhou, X. Kuang, K. Lin, Y. Cao, *et al.*, Intrinsic-strain-induced ferroelectric order and ultrafine nanodomains in SrTiO<sub>3</sub>, *Proc. Natl. Acad. Sci. U.S. A.* **121**, e2400568121 (2024).
- [36] A. Antons, J. Neaton, K. M. Rabe, and D. Vanderbilt, Tunability of the dielectric response of epitaxially strained SrTiO<sub>3</sub> from first principles, *Phys. Rev. B* **71**, 024102 (2005).
- [37] A. Vasudevarao, A. Kumar, L. Tian, J. Haeni, Y. Li, C.-J. Eklund, Q. Jia, R. Uecker, P. Reiche, K. Rabe, *et al.*,

- Multiferroic domain dynamics in strained strontium titanate, *Phys. Rev. Lett.* **97**, 257602 (2006).
- [38] R. F. Berger, C. J. Fennie, and J. B. Neaton, Band gap and edge engineering via ferroic distortion and anisotropic strain: The case of SrTiO<sub>3</sub>, *Phys. Rev. Lett.* **107**, 146804 (2011).
- [39] T. Angsten and M. Asta, Epitaxial phase diagrams of SrTiO<sub>3</sub>, CaTiO<sub>3</sub>, and SrHfO<sub>3</sub>: Computational investigation including the role of antiferrodistortive and a-site displacement modes, *Phys. Rev. B* **97**, 134103 (2018).
- [40] N. Pertsev, A. Tagantsev, and N. Setter, Phase transitions and strain-induced ferroelectricity in SrTiO<sub>3</sub> epitaxial thin films, *Phys. Rev. B* **61**, R825 (2000).
- [41] Y. Li, S. Choudhury, J. Haeni, M. Biegalski, A. Vasudevarao, A. Sharan, H. Ma, J. Levy, V. Gopalan, S. Trolier-McKinstry, *et al.*, Phase transitions and domain structures in strained pseudocubic (100) SrTiO<sub>3</sub> thin films, *Phys. Rev. B* **73**, 184112 (2006).
- [42] G. Sheng, Y. Li, J. Zhang, S. Choudhury, Q. Jia, V. Gopalan, D. G. Schlom, Z. Liu, and L. Chen, Phase transitions and domain stabilities in biaxially strained (001) SrTiO<sub>3</sub> epitaxial thin films, *J. Appl. Phys.* **108** (2010).
- [43] R. He, H. Wu, L. Zhang, X. Wang, F. Fu, S. Liu, and Z. Zhong, Structural phase transitions in SrTiO<sub>3</sub> from deep potential molecular dynamics, *Phys. Rev. B* **105**, 064104 (2022).
- [44] L. Han, G. Dong, M. Liu, and Y. Nie, Freestanding perovskite oxide membranes: a new playground for novel ferroic properties and applications, *Adv. Funct. Mater.* **34**, 2309543 (2024).
- [45] See Supplemental Material, which includes Refs. [46- 57], computational details of DFT, Modulated ground state for SrMnO<sub>3</sub>; Potential energy surface of individual and coupled modes; Polarization dependent magnetization deviation; Strain and polarization fields in lower-energy modulated BiFeO<sub>3</sub> and PbTiO<sub>3</sub>.
- [46] G. Kresse and J. Hafner, Ab initio molecular dynamics for liquid metals, *Phys. Rev. B* **47**, 558 (1993).
- [47] P. E. Blöchl, Projector augmented-wave method, *Phys. Rev. B* **50**, 17953 (1994).
- [48] J. P. Perdew and A. Zunger, Self-interaction correction to density-functional approximations for many-electron systems, *Phys. Rev. B* **23**, 5048 (1981).
- [49] J. P. Perdew, A. Ruzsinszky, G. I. Csonka, O. A. Vydrov, G. E. Scuseria, L. A. Constantin, X. Zhou, and K. Burke, Restoring the density-gradient expansion for exchange in solids and surfaces, *Phys. Rev. Lett.* **100**, 136406 (2008).
- [50] A. Liechtenstein, V. I. Anisimov, and J. Zaanen, Density-functional theory and strong interactions: Orbital ordering in mott-hubbard insulators, *Phys. Rev. B* **52**, R5467 (1995).
- [51] J. Guo, P. Wang, Y. Yuan, Q. He, J. Lu, T. Chen, S. Yang, Y. Wang, R. Erni, M. Rossell, *et al.*, Strain-induced ferroelectricity and spin-lattice coupling in SrMnO<sub>3</sub> thin films, *Phys. Rev. B* **97**, 235135 (2018).
- [52] B. F. Grosso and N. A. Spaldin, Prediction of low-energy phases of BiFeO<sub>3</sub> with large unit cells and complex tilts beyond glazer notation, *Phys. Rev. Mater.* **5**, 054403 (2021).
- [53] H. J. Monkhorst and J. D. Pack, Special points for brillouin-zone integrations, *Phys. Rev. B* **13**, 5188 (1976).
- [54] A. Togo and I. Tanaka, First principles phonon calculations in materials science, *Scr. Mater.* **108**, 1 (2015).
- [55] H. T. Stokes, D. M. Hatch, B. J. Campbell, and D. E. Tanner, Isodisplace: a web-based tool for exploring structural distortions, *J. Appl. Crystallogr.* **39**, 607 (2006).
- [56] H. Fu and L. Bellaïche, First-principles determination of electromechanical responses of solids under finite electric fields, *Phys. Rev. Lett.* **91**, 057601 (2003).
- [57] R. Resta, Macroscopic polarization in crystalline dielectrics: the geometric phase approach, *Rev. Mod. Phys.* **66**, 899 (1994).
- [58] R. Cowley, Acoustic phonon instabilities and structural phase transitions, *Phys. Rev. B* **13**, 4877 (1976).
- [59] G. Guzmán-Verri, C. Liang, and P. Littlewood, Lamellar fluctuations melt ferroelectricity, *Phys. Rev. Lett.* **131**, 046801 (2023).
- [60] J. H. Lee and K. M. Rabe, Epitaxial-strain-induced multiferroicity in SrMnO<sub>3</sub> from first principles, *Phys. Rev. Lett.* **104**, 207204 (2010).
- [61] C. Cazorla, M. Stengel, J. Íñiguez, and R. Rurali, Giant multiphononic effects in a perovskite oxide, *Npj Comput. Mater.* **9**, 97 (2023).
- [62] S. Li, Y. Zhu, Y. L. Tang, Y. Liu, S. Zhang, Y. Wang, and X. Ma, Thickness-dependent  $a_1/a_2$  domain evolution in ferroelectric PbTiO<sub>3</sub> films, *Acta Mater.* **131**, 123 (2017).
- [63] Y. Wang, Y. Tang, Y. Zhu, Y. Feng, and X. Ma, Converse flexoelectricity around ferroelectric domain walls, *Acta Mater.* **191**, 158 (2020).